J Mol Model (2013) 19:2127–2142
DOI 10.1007/s00894-012-1684-9

ORIGINAL PAPER

Investigation of the antioxidant properties of hyperjovinol A through its Cu(II) coordination ability

Liliana Mammino

Received: 30 April 2012 / Accepted: 6 November 2012 / Published online: 5 December 2012

Abstract Hyperjovinol A (2-methyl-1-(2,4,6-trihydroxy-3-(3-hydroxy-3,7-dimethyloct-6-enyl)phen yl)propan-1-one) is an acylated phloroglucinol isolated from *Hypericum Jovis* and exhibiting antioxidant properties comparable with those of the most common antioxidant drugs. The study models the compound's antioxidant ability through its ability to coordinate a Cu^{2+} ion and reduce it to Cu^{+}. Complexes with a Cu^{2+} ion were calculated for all the low energy and for representative high energy conformers of hyperjovinol A, placing the ion in turn near each of the electron-rich binding sites. The most stable complexes are those in which Cu^{2+} binds simultaneously to the O of the OH in the geranyl-type chain (R′) and the C═C double bond at the end of R′, or to the O of a phenol OH and the O of the OH in R′. The most stable complexes in which Cu^{2+} binds only to one site are those in which it binds to the C═C double bond at the end of R′ or to the sp^2 O of the $COCH(CH_3)_2$ acyl group. Cu^{2+} is reduced to Cu^{+} in all complexes. Comparisons with corresponding complexes of other molecular structures in which one or more of the structural features of hyperjovinol A are modified attempt to elucidate the role, for the antioxidant ability, of relevant features of hyperjovinol A, like the presence and position of the OH or the C═C double bond in R′. Calculations at the DFT/B3LYP/6–31+G(d,p) level were performed for all the structures considered. Calculations utilizing the LANL2DZ pseudopotential for the Cu^{2+} ion were also performed for hyperjovinol A.

Keywords Acylphloroglucinols · Antioxidant activity · Hyperjovinol A · Hyperjovinol A-Cu^{2+} complexes · Polyphenolic compounds

Introduction

Hyperjovinol A (2-methyl-1-(2,4,6-trihydroxy-3-(3-hydroxy-3,7-dimethyloct-6-enyl)phenyl)-propan-1-one, hereafter denoted by the acronym HPJ-A) is a naturally-occurring acylphloroglucinol isolated from *Hypericum Jovis* [1] and exhibiting antioxidant ability comparable to that of the commonly used antioxidant standard Trolox (6-hydroxy-2,5,7,8-tetramethylchroman-2-carboxylic acid, a water-soluble form of vitamin E) [1, 2]. The interest in antioxidant compounds is continuously increasing because they offer protection against reactive oxygen species (ROS), whose excess production may cause damage to the central nervous system and appears to be implicated in the pathogenesis of various neurodegenerative diseases, including ischemia, Alzheimer disease, Parkinson disease and schizophrenia [1–4]. Compounds from natural sources utilized in traditional medicine have the advantage of proved compatibility with a living organism, which favors their ability to reach their target and exert an action within an organism; this motivates the increasing attention to their potentialities for drug development. The understanding of the molecular origin of the activity of naturally-occurring compounds can help design compounds with more potent activity [5]. It is thus important to understand the influence of as many molecular details as possible on the activity of naturally occurring compound.

Phenolic compounds are plant secondary metabolites commonly found in herbs, fruits, vegetables, cereals, tea, coffee, wine, etc. [6]. Several of them exhibit antioxidant activity, whose possible mechanisms have been the object of

Electronic supplementary material The online version of this article (doi:10.1007/s00894-012-1684-9) contains supplementary material, which is available to authorized users.

L. Mammino (✉)
Department of Chemistry, University of Venda, P/bag X5050, Thohoyandou 0950, South Africa
e-mail: sasdestria@yahoo.com

intensive studies [6–15]. The antioxidant activity, generally linked to the phenol OH, appears to be enhanced by the presence of two ortho OH, whose intramolecular hydrogen bond (IHB) contributes to stabilize the radical form of the molecule resulting from antioxidant action [7, 9], and also by the presence of a C=C double bond in a suitable position [7, 9].

In acylphloroglucinols (ACPLs, phloroglucinol derivatives with a COR group attached to the ring), the presence of three phenol OH is expected to confer good antioxidant properties, and they have been proposed as potentially interesting lead compounds for the development of drugs for the treatment of degenerative diseases [16]. Although the three phenol OH, being mutually meta, cannot H-bond to each other, the sp^2 O in the COR group can form a comparatively strong IHB with either of the ortho OH [17–19], which may have roles analogous to those of ortho-OH IHBs in enhancing antioxidant activity.

Despite their reported pharmaceutical properties, antioxidant ACPLs have not yet been the object of systematic theoretical studies, not even within ample reviews of antioxidant polyphenols like [12]. The current work pertains to an ongoing systematic computational study of antioxidant ACPLs.

Figure 1 shows the structure of the HPJ-A molecule and the atom numbering utilized in this work. The numbering pursues maximum consistency with that utilized in previous studies of ACPLs [17–19], to facilitate comparisons with the general features identified for ACPLs, like geometry preferences and IHB patterns. In HPJ-A, R is an isopropyl group and the substituent at C3 (here concisely termed R′) is $CH_2CH_2COH(CH_3)CH_2CH_2CHC(CH_3)_2$, a geranyl-type chain without the C=C double bond closer to the ring and with an OH on the third C atom from the ring. It is noteworthy that all ACPLs reported to have interesting antioxidant activity contain either additional OH with respect to the phloroglucinol moiety or additional C=C double bonds in some substituents. This motivates the investigation of the possible roles of these additional functions in strengthening the molecule's activity.

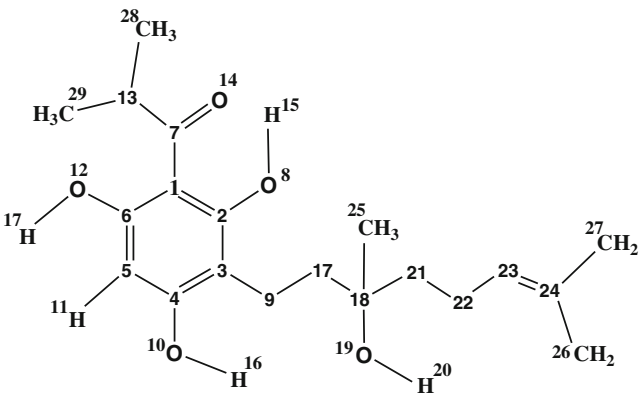

Fig. 1 Structure of hyperjovinol A and atom numbering utilized in this work. The atom numbering of the phloroglucinol moiety and other relevant atoms maintains the numbering utilized in previous works on acylphloroglucinols [17–19, 37] to facilitate possible cross-references

The current study models the antioxidant ability of HPJ-A through its ability to coordinate a Cu^{2+} ion and reduce it to Cu^{+} [5, 20]. The chelation of metals may be one of the mechanisms of the antioxidant activity of polyphenols [6]. Although there is not yet conclusive information as to whether this concerns antioxidant ACPLs, the possibility that metal chelation may actually be part of the mechanism increases the interest of the study.

Complexes of biomolecules with Cu^{2+} have been objects of various studies in the last decades, because of the role of Cu^{2+} in bioprocesses and because of its suitability for models involving a metal dication [21]. Its possible role as catalysts for the formation of peptide bonds in aqueous solution, and the presence of Cu^{2+} ions in the active site of some proteins, has prompted studies of its complexes with aminoacids [22–27]. Other works investigated complexes of Cu^{2+} with DNA/RNA bases like uracil and its derivatives [28–31] or adenine-thymine [32], as well as with other ligands [33].

The HPJ-A molecule contains six sites apt for binding Cu^{2+}: the five O atoms and the C23=C24 double bond. The strength of the molecule-ion interaction in the complexes provides indications of Cu^{2+} binding preferences for the different sites. Forty seven complexes were calculated, considering different geometries of the HPJ-A moiety and different binding sites for each geometry. The results show greater preference for Cu^{2+} to bind simultaneously to the OH in R′ (O19) and the C23=C24 double bond, or to the O of a phenol OH (O8 or O10) and O19. When binding only to one site, it prefers to bind to the C23=C24 double bond and, secondly, to O14. In all the complexes investigated, the charge on the Cu ion decreases to less than +1, proving the ability of HPJ-A to reduce Cu^{2+} to Cu^{+}; in this way, the modeling with the Cu^{2+} ion accounts for the antioxidant ability of HPJ-A.

Further elucidation of the roles of individual sites and of the possibility of mutual influences was attempted by considering complexes of other molecular structures (24 different ones) expected to enable significant "isolation" of possible influences by one or the other site, or by specific structural features, on the molecule's ability to bind Cu^{2+} and reduce its charge.

Calculations in solution were carried out to investigate whether and how the HPJ-A ability to reduce Cu^{2+} may vary in solution.

Tables with detailed results (including natural orbital occupancies of Cu, spin densities of the O and H atoms of the OH groups and of C22 and C23, charges on all the O atoms and on the hydroxyl H atoms, comparisons of IHB

parameters in the isolated HPJ-A molecule and in the complexes, extensive comparisons with the results obtained for the additional molecular structures considered, results in solution, etc.) and figures showing all interesting geometries and other graphic information (electron density and spin density maps, the shapes of HOMOs), are included in the Supporting material.

Computational details

A conformational study of uncomplexed HPJ-A was preliminarily carried out, utilizing the information from the study of ACPLs [17–19] as a guideline for the conformational search. Complexes with a Cu^{2+} ion attached to different binding sites (including simultaneous binding to two sites when geometrically possible) were calculated for all the low energy conformers of HPJ-A and for selected high energy ones, resulting in a sufficiently representative (although not exhaustive) investigation of HPJ-A—Cu^{2+} complexes.

Calculations were performed with the density functional theory (DFT) method, using the B3LYP functional [34–36] and the 6–31+G(d,p) basis set, as a reasonable compromise between result accuracy and computational affordability, and also to maintain the possibility of comparison with relevant results obtained with the same method for ACPLs [17–19, 37]. The use of diffuse and polarization functions is important for a better description of IHBs [23] and had proved relevant for the quality of DFT/B3LYP results for ACPLs [17–19, 37]. All the calculations in vacuo were performed with full optimization (fully relaxed geometry), to obtain the best information on conformational preferences and the best evaluation of the interaction between HPJ-A and Cu^{2+}. The unrestricted approach was used for the complexes (open shell).

The HPJ-A—Cu^{2+} complexes were calculated also using B3LYP/6–31+G(d,p) for the C, O and H atoms and the LANL2DZ pseudopotential [38] for Cu^{2+}, since this enables better estimation of the molecule-ion interaction for transition metals complexes [39, 40].

Some studies [25, 32, 41] have shown that the BHLYP functional performs better for complexes with the Cu^{2+} cation. However, the difference between B3LYP and BHLYP results may depend on the molecular system and on the features considered [25], and the two functionals provide similar geometry parameters [25]. Furthermore, B3LYP still represents the most widely used density functional; its performance in determining some chemical properties is usually accepted [6] and its results are reasonable [32]; geometry determinations appear reliable [6, 12], and it has been considered suitable in many studies of metal-ion complexes (e.g., [5, 10, 20, 23, 24, 30, 31, 42, 43]).

Although B3LYP tends to overestimate the binding energies when Cu^{2+} is involved, it was shown [20] that the relative stabilities of the complexes and the binding energies values remain fairly comparable among themselves, thus being suitable [20] and widely utilized [13] for comparison purposes. Since this study focuses mostly on comparisons across complexes (comparison of the binding abilities of different sites, of charges, of corresponding complexes of different structures, etc.), B3LYP can be considered adequate. A detailed comparison of the B3LYP and BHLYP performance specifically for the complexes of ACPLs with Cu^{2+} may be worthy of a separate study, after the investigation of other relevant antioxidant ACPLs is completed (different methods may perform differently with different classes of compounds; e.g., for ACPLs, HF results were found to be more in agreement than DFT results with MP2 results [17–19]).

Natural bond orbital [44–48] analysis was utilized to get more detailed information about the electronic structure. Natural charges on the atoms are particularly important, as the reduction of the charge of the Cu^{2+} ion in the complex is an indication of the ligand's ability to reduce an oxidant species.

The molecule-ion interaction energy (MIIE) was calculated using the equation [20]:

$$\mathrm{MIIE} = \mathrm{E_{complex}} - \mathrm{E_{ligand}} - \mathrm{E_{ion}}, \quad (1)$$

where $E_{complex}$ is the energy of the complex, E_{ligand} is the energy of the isolated molecule and E_{ion} is the energy of the isolated Cu^{2+} ion.

Basis set superposition error (BSSE) corrections were not included in the calculation of MIIE because this error is usually small for DFT methods when the basis set expansion is sufficiently flexible [30, 49]. Moreover, while counterpoise corrections can be important for interactions between neutral molecules (e.g., H-bonding with water), they appear to be almost non influential for large interaction energies, above all when the main purpose is comparative [20], like in the present work.

Harmonic vibrational frequencies were calculated, at the same level of theory, for a representative number of complexes (including all the lower energy ones) to characterize them as minima or saddle point and to estimate MIIE corrected for zero point energy (ZPE).

Calculations in solution considered the same solvents − chloroform, acetonitrile and water − utilized in the general studies of ACPLs [17–19]. These solvents cover the polarity and H-bonding ability ranges of the media in which a molecule may preferably be present within a living organism (acetonitrile is also a good model for the medium in membranes). Although non-polar solvents may not be the most apt for the investigation of actual Cu^{2+} binding (as Cu^{2+} would prefer polar media), in the current study complexes with Cu^{2+} are utilized to model the ability for an activity

which, within living organisms, occurs through more complex mechanisms. The consideration of less polar or non-polar solvents is justified by the high probability that HPJ-A molecules are more extensively present in non-polar media in a living organism (the octanol/water partition coefficient is 3.83845); therefore, it becomes important to evaluate whether HPJ-A maintains its ability to reduce Cu^{2+} in less polar or non-polar media.

Calculations in solution utilized the polarizable continuum model (PCM, [50, 51]), where the solute is embedded in a cavity built from intersecting sphere and surrounded by a continuum solvent. The default settings of the Gaussian03 package [52] were utilized: IEF (integral equation formalism model, [53–56]) and average tesserae area 0.200 $Å^2$ for the surface of the cavity around the solute. The UAHF radii (united atom topological model applied on radii optimized for the HF/6–31G(d) level) were utilized for the spheres. The dielectric constants are: 4.90 for chloroform, 36.64 for acetonitrile and 78.39 for water. PCM calculations were performed as single point on in-vacuo-optimized geometries, at the same level of theory, because of affordability reasons in view of the computational demands of the PCM optimization algorithm for molecular systems of the size considered. The study of ACPLs [17] has shown good consistency between the results of full-reoptimization and single point PCM calculations, above all for the identification of trends.

A better model for the description of the complexes in water solution would involve the inclusion of explicit water molecules in the vicinity of the metal ion and the use of PCM on the resulting supermolecular structure [21, 57–59] or, even better, including also explicit water molecules attached to the H-bond donor/acceptor sites of HPJ-A, along the patterns identified for adducts of ACPLs with explicit water molecules. However, the calculation of HPJ-A—Cu^{2+} complexes including explicit water molecules in the vicinity of the Cu ion already proved excessively costly (practically unaffordable) in terms of computational time.

All the calculations were performed using Gaussian 03, Revision D 01 [52].

All the energy values reported are in kcal mol^{-1} and all the distances are in Å.

Results

Conformational preferences of the hyperjovinol A molecule

Figure 2 shows the calculated conformers of the HPJ-A molecule and the symbols utilized to denote them in order to keep track of their geometry characteristics; the symbols follow the main patterns introduced for ACPLs [17–19], to facilitate references to general properties of ACPLs. The sp^2 O of COR (O14) can form an IHB ("first IHB", [17–19]) with either of the ortho OH, i.e., H15 or H17. The OH in R′ can form a "second IHB" [37], in which O19 is acceptor to either H15 or H16. The stability patterns are fully consistent with those identified for ACPLs in general [17] and for ACPLs in which R′ contains a group capable of forming a second IHB [37] in particular: preference for the simultaneous presence of two IHBs; preference for the first IHB to form on the same side as R′; preference for uniform orientation of the three phenol OH, in line with the parent compound preference for C_{3h} symmetry [60]. Differently from other ACPLs in which R′ contains an OH, the only second IHBs present are those in which a phenol O is donor to O19; geometries in which H20 is donor to either O8 or O10 appear to be non-viable (the inputs optimize to something else), likely because of the combined effects of the general preference of phenol OH to be H-bond donors and of some effects related to the position of the OH in R′.

Results for the complexes of the hyperjovinol A molecule in vacuo

Complexes of HPJ-A with a Cu^{2+} ion were calculated for the best conformers of HPJ-A, considering all the possible coordination sites (O8, O10, O12, O14, O19 and the C23=C24 π bond) individually, and also simultaneous coordination to two sites when geometrically possible. Simultaneous coordination is possible for the following pairs of sites: O19 and the C23=C24 π bond; O19 and either O8 or O10, when the second IHB is not present; off-plane O14 and either O8 or O12 for the high-energy conformers without the first IHB. Complexes of higher energy conformers were calculated to verify whether the relative stabilities of the complexes might differ substantially from the relative stabilities of the conformers of isolated HPJ-A. In particular, representative complexes of conformers without the first IHB were calculated to verify the possible stabilizing effect of Cu^{2+} binding simultaneously to O14 and either O8 or O12.

The complexes are denoted with the acronym identifying the HPJ-A conformer (Fig. 2) followed by "Cu" and, in parentheses, the position/s to which Cu^{2+} binds. When Cu^{2+} binds simultaneously to two O atoms, both atoms are indicated, with the phenol O appearing before another O. The symbol "pi" indicates that Cu^{2+} binds to the C23=C24 π bond. Figure 3 shows a selection of complexes with the best relative energy and MIIE and Fig. 4 shows the corresponding spin density maps. Table 1 reports the complexes' relative energy (ΔE), the MIIE values, the charge on Cu (both from natural orbital analysis and Mulliken), the Mulliken Cu spin density and the Cu distance from the O atom/s to which it binds. Table 2 reports the ZPE-corrected MIIE for a representative selection of complexes.

The HPJ-A geometry in the complex is very close to that of a stable conformer of isolated HPJ-A for Cu^{2+} coordination at

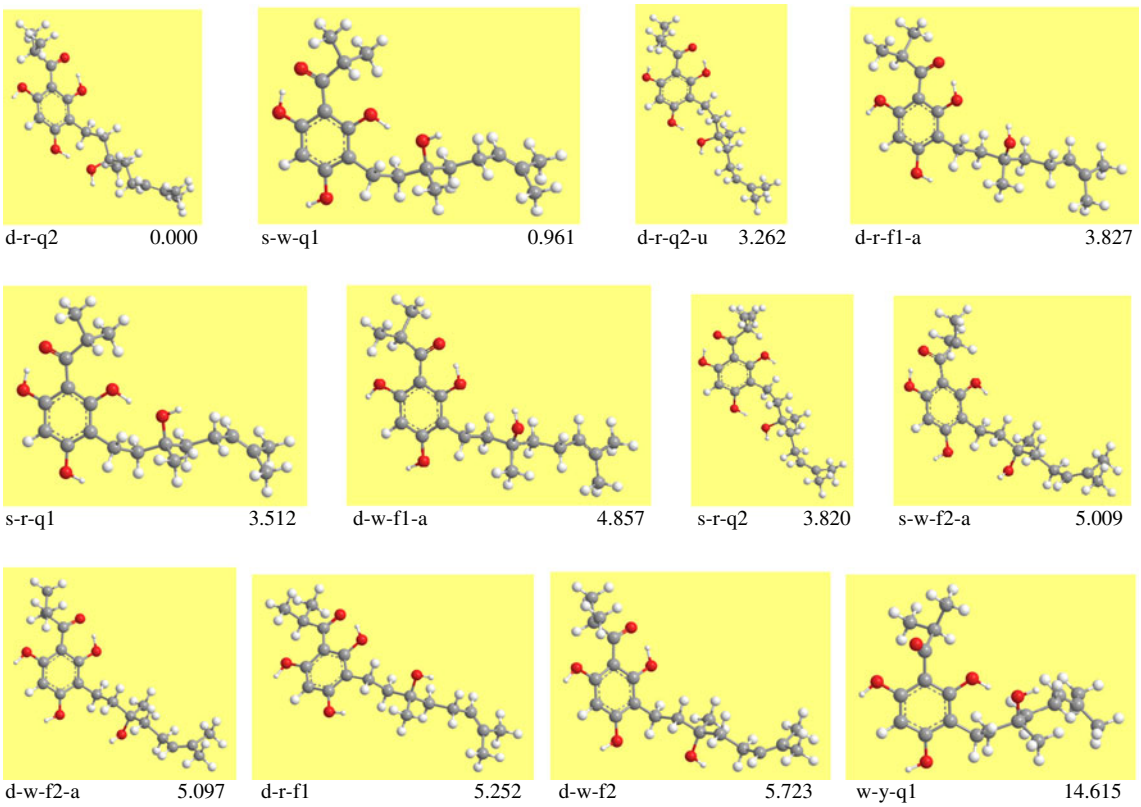

Fig. 2 Conformational preferences of the isolated hyperjovinol A molecule. The figure shows the most representative conformers of hyperjovinol A, from full-optimization DFT/B3LYP/6–31+G(d,p) results in vacuo. Under each image, the acronym used to denote the given conformer is reported on the left hand side and the conformer's relative energy (kcal mol^{-1}) on the right hand side. The meaning of the individual letters in the acronyms [17–19] is the following: **d** informs that the first IHB is on the same side as R′ and **s** that it is on the other side; **r** informs that H16 is oriented toward R′ and **w** that it is oriented toward the other side; **q1** informs that the second IHB engages H15 and O19, and **q2** that it engages H16 and O19; **f** informs that the second IHB is not present, followed by **1** if it corresponds to H15···O19 removal and by **2** if it corresponds to H16···O19 removal, and also by **a** when H20 is oriented "toward us"; **u** informs that H15 or H17, not engaged in the first IHB, is oriented toward R. For conformers without the first IHB, the acronym does not contain the letters d or s; the letter **x** informs that off-plane O14 is oriented "to the right" and the letter **y** that it is oriented "to the left"

certain sites, whereas it takes features that are not encountered in stable conformers of isolated HPJ-A for other coordination sites. It is very close when Cu^{2+} is placed in the vicinity of O14, or of O8 or O12 when not engaged in the first IHB, or near O10 when the H15···O19 second IHB is also present. If Cu^{2+} is placed in the vicinity of the O that is donor to the first IHB, the first IHB does not break, but the proton transfers to O14 (gets closer to O14 than to O8 or O12) and Cu^{2+} binds to the phenol O. A similar proton transfer occurs when Cu^{2+} binds to the C23=C24 π bond, or when Cu^{2+} binds to O10 and O19 simultaneously and the first IHB is on the right (d-type conformers).

When Cu^{2+} binds simultaneously to O19 and the C23=C24 π bond, or only to O19 or to O10 in conformers with the first IHB on the right and no second IHB (d-f1-type conformers), it causes the formation of the H20···O8 second IHB, resulting in two consecutive IHBs in which O8 is donor for the first IHB and acceptor for the second. Such a second IHB, in which H20 is donor to a phenol O, is not encountered in stable conformers of isolated HPJ-A. Its presence is denoted by v1 in the conformer portion of the complex name [37]. H20···O8 is shorter when Cu^{2+} binds to O19 and longer when it binds to O10. It is difficult to evaluate its stabilizing effect. It is present in the lowest energy complex (d-w-v1-Cu(O19,pi)) and the corresponding one with opposite orientation of O10–H16 (d-r-v1-Cu(O19pi)), where, however, the greatest stabilizing effect is due to Cu^{2+} binding to the C23=C24 π bond. The other complexes in which H20···O8 is present have high relative energy and comparatively poor MIIE.

When Cu^{2+} is placed in the vicinity of a second IHB, in the region between the O and H atoms forming it, the H atom rotates to the other side on optimization, breaking the second IHB; Cu^{2+} binds to the two O atoms, and the HPJ-A geometry changes to that of a stable conformer without the second IHB (f1- or f2-type). When Cu^{2+} binds simultaneously to O8 and O19 and the first IHB engages H17 (s-type conformers), H15 rotates upward (yielding the corresponding u-type conformer) for s-w and rotates 49.2° off-plane for s-r; this difference highlights the general

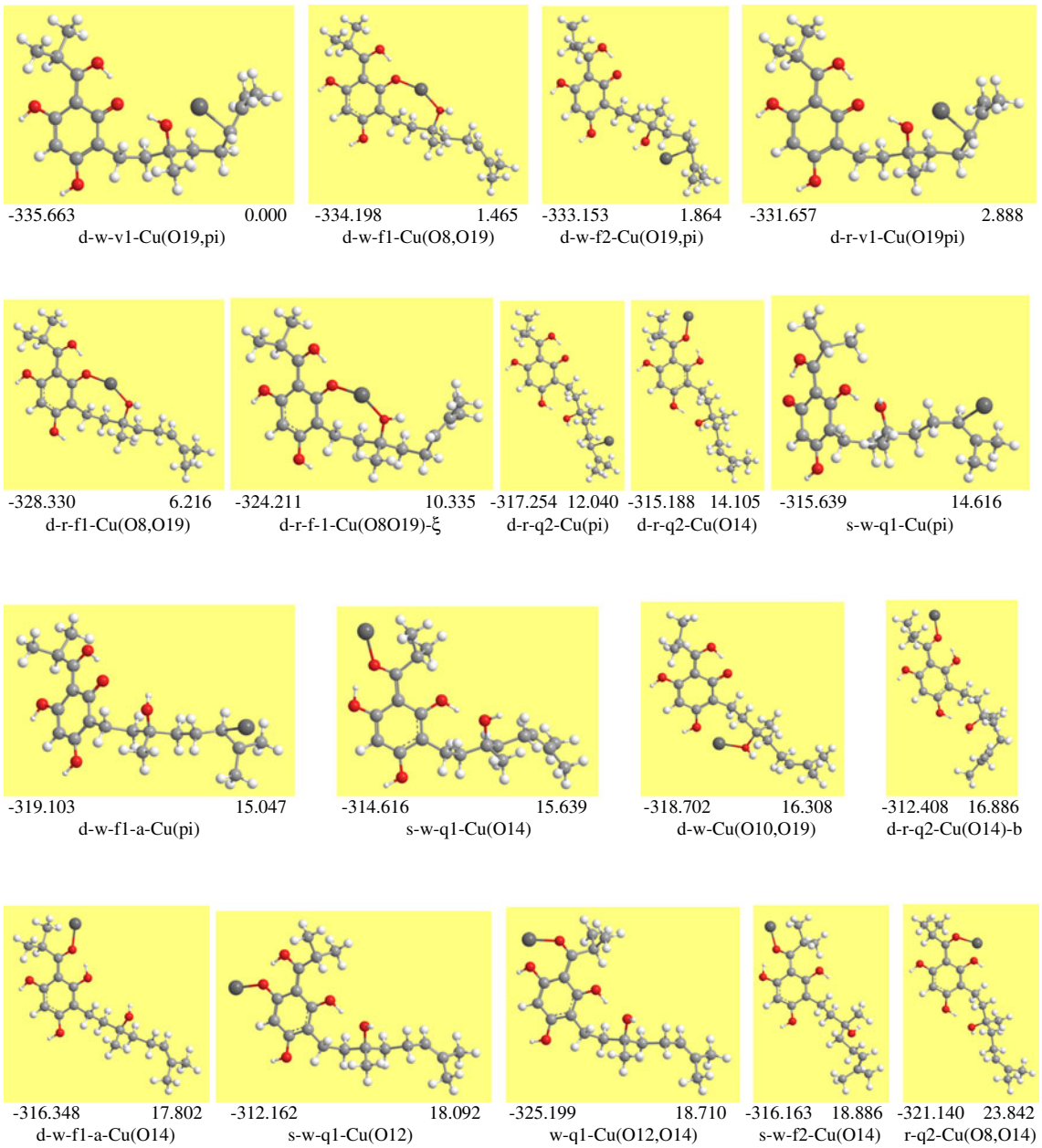

Fig. 3 Representative complexes of hyperjovinol A with a Cu^{2+} ion. The figure shows complexes representative of different geometries, selected among those with best molecule-ion interaction energy (MIIE) in vacuo and arranged in order of increasing relative energy (ΔE). The value of MIIE (kcal mol^{-1}, not corrected for ZPE or BSSE) is reported under each image on the left and the values of ΔE (kcal mol^{-1}) on the right. The results are from full-optimization DFT/B3LYP calculations with the 6–31+G(d,p) basis set for the C, O and H atoms and the LANL2DZ pseudopotential for the Cu^{2+} ion

importance of the orientation of all the phenol OHs, including those that are not directly binding Cu or in its vicinity, as is O10H16 in this case.

In the estimation of MIIE (Eq. 1), E_{ligand} was taken as the energy of the isolated HPJ-A conformer closest to the geometry that HPJ-A has in the given complex. The estimation is uncomplicated when the optimization does not bring major geometry changes, or the changes yield a geometry of the HPJ-A moiety close to that of another stable conformer of uncomplexed HPJ-A. It may require some reflections when the HPJ-A geometry in the complex contains features that are not present in any conformer of uncomplexed HPJ-A and that are not maintained on removing Cu^{2+} from the complex and relaxing the HPJ-A geometry. This occurs both when there is a proton transfer (from O8 or O12 to O14) in the complex and when there is the formation of the second H20···O8 IHB. These two cases, therefore, deserve some closer analysis.

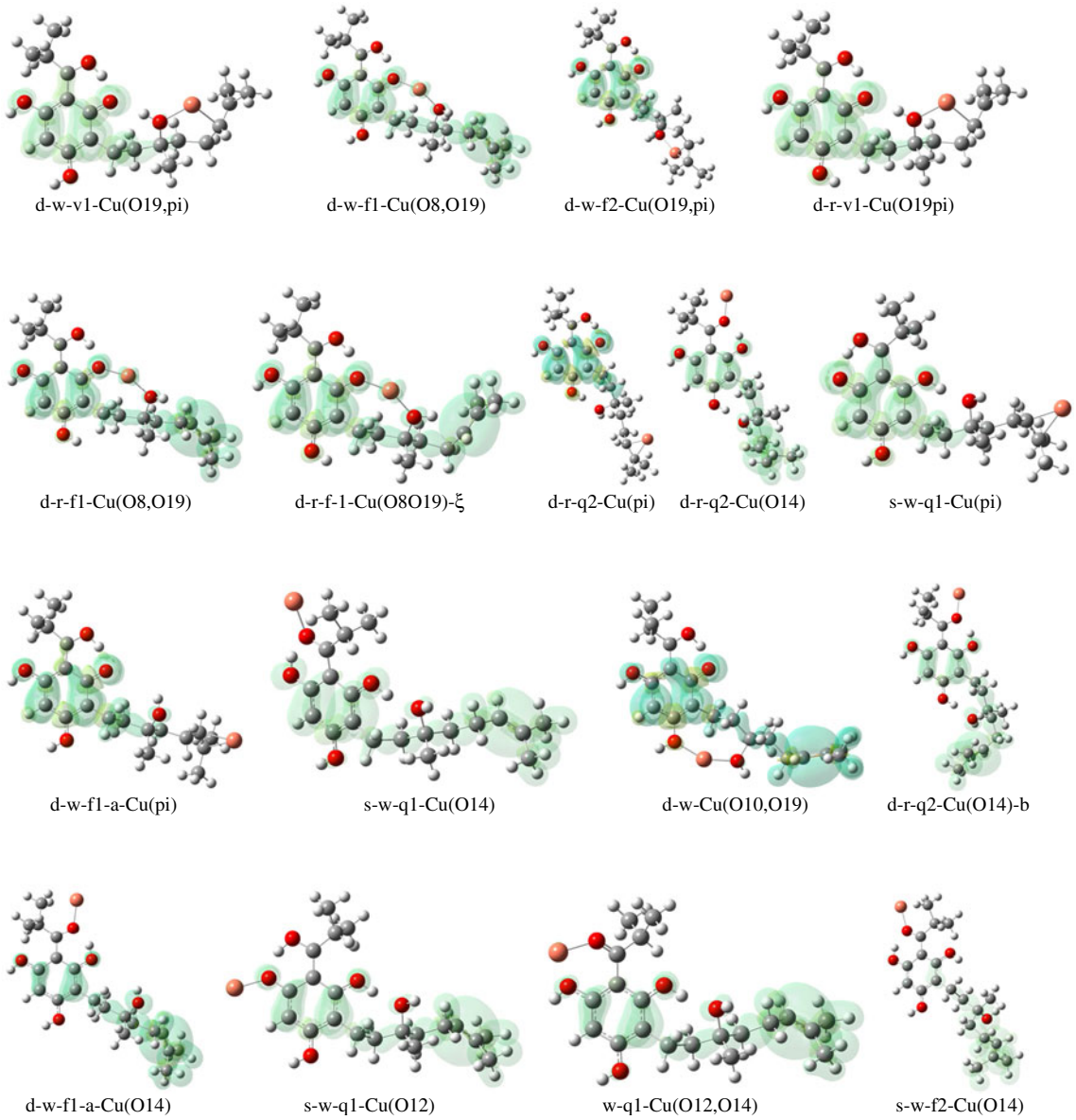

Fig. 4 Spin density maps for the complexes of hyperjovinol A with a Cu^{2+} ion shown in Fig. 3. Results from full-optimization DFT/B3LYP calculations with the 6–31+G(d,p) basis set for the C, O and H atoms and the LANL2DZ pseudopotential for the Cu^{2+} ion. The table below shows the ranges of values, to be taken as between $-a \times 10^{-3}$ and $+a \times 10^{-3}$:

complex	a	complex	a	complex	a
d-w-v1-Cu(O19,pi)	3.016	d-r-q2-Cu(pi)	1.131	d-r-q2-Cu-O14-b	2.573
d-w-f1-Cu(O8,O19)	1.916	d-r-q2-Cu(O14)	2.386	d-w-f1-a-Cu(O14)	1.673
d-w-f2-Cu-(O19,pi)	1.542	s-w-q1-Cu(pi)	2.505	s-w-q1-Cu(O12)	2.853
d-r-v1-Cu(O19,pi)	2.586	d-w-f1-a-Cu(pi)	1.763	w-q1-Cu(O12,O14)	2.417
d-r-f1-Cu(O8,O19)	1.664	s-w-q1-Cu(O14)	2.867	s-w-f2-Cu(O14)	3.958
d-r-f1-Cu(O8,O19)-ξ	1.901	d-w-Cu(O10,O19)	1.192		

When the only difference with a stable conformer of isolated HPJ-A is the proton transfer from O8 or O12 to O14, the MIIE evaluation utilizing the corresponding stable conformer of isolated HPJ-A (with the proton closer to O8 or O12) as reference for E_{ligand} can be considered sufficiently reliable because of the similarities of the two cases. What used to be termed the "resonance assisted" [61, 62] character of the first IHB is maintained. The first IHB in the two cases (with and without the proton transfer) corresponds to one or the other of the two minima along the donor-acceptor O···O distance and, therefore, their energy difference should not be so relevant as to significantly affect MIIE estimations.

The accuracy of MIIE estimation may be slightly more uncertain for the cases in which the H20···O8 second IHB

Table 1 Relevant quantities for the complexes of hyperjovinol A with a Cu^{2+} cation: complex relative energy, molecule- metal ion interaction energy, charge on the Cu atom (both from natural population analysis and Mulliken charge), Cu atom spin density and Cu···O distances. DFT/B3LYP results in vacuo with the 6–31+G(d,p) basis set for the C, O and H atoms and the LANL2DZ pseudopotential for the Cu^{2+} ion

Complex	Relative energy (kcal mol^{-1})	Molecule-ion interaction energy (kcal mol^{-1})	Charge on Cu in the complex		Cu atomic spin density (Mulliken)	Cu···O distance [a] (Å)	
			Natural	Mulliken		first O	second O
d-w-v1-Cu(O19,pi)	0.000	−335.663	0.88003	0.10573	0.000655	1.993 [b]	
d-w-f1-Cu(O8,O19)	1.465	−334.198	0.87859	0.29723	0.017933	1.915	1.966
d-w-f2-Cu(O19,pi)	1.864	−333.153	0.87547	0.14109	0.000085	2.018 [c]	
d-r-v1-Cu(O19pi)	2.888	−331.657	0.87985	0.10762	0.000545	1.997 [d]	
d-r-f1-Cu(O8,O19)	6.216	−328.330	0.88078	0.31217	0.016130	1.913	1.965
s-w-f1-u-Cu(O19pi)	6.548	−330.976	0.88284	0.14660	0.000139	2.016 [e]	
s-w-f1-a-Cu(O19pi)	7.935	−326.367	0.87967	0.14823	−0.000055	2.026 [f]	
d-r-f1-Cu(O8O19)-ξ	10.335	−324.211	0.89450	0.33028	0.029258	1.923	1.944
d-r-q2-Cu(pi)	12.040	−317.254	0.82898	0.33515	0.000011	– [g]	
d-r-q2-Cu(O14)	14.105	−315.188	0.93753	0.48411	−0.000015	1.968	
s-w-q1-Cu(pi)	14.616	−315.639	0.85454	0.32421	0.000116	– [h]	
d-w-f1-a-Cu(pi)	15.047	−319.103	0.85154	0.32008	0.000516	– [i]	
s-w-q1-Cu(O14)	15.639	−314.616	0.93935	0.51606	−0.000018	1.964	
d-w-Cu(O10,O19)	16.308	−318.708	0.88260	0.41052	0.001352	1.998	1.955
d-r-q2-Cu(O14)-b	16.886	−312.408	0.93758	0.48289	−0.000020	1.968	
d-w-f1-a-Cu(O14)	17.802	−316.348	0.93607	0.48220	−0.000007	1.965	
s-w-q1-Cu(O12)	18.092	−312.162	0.91356	0.65516	0.001166	1.900	
d-w-Cu(O10,O19)-b	18.645	−317.018	0.88371	0.42118	0.000340	1.999	1.954
w-q1-Cu(O12,O14)	18.710	−325.199	0.93969	0.61807	0.001810	2.172	1.956
s-w-f2-Cu(O14)	18.886	−316.163	0.93621	0.49990	0.000023	1.959	
s-r-q2-Cu(O14)	19.482	−313.632	0.93807	0.50569	−0.000034	1.966	
s-r-q1-Cu(O14)	20.113	−312.693	0.94005	0.51973	−0.000078	1.964	
d-r-f1-a-Cu(O14)	20.129	−312.991	0.93554	0.48315	−0.000009	1.966	
s-r-q1-Cu(O12)	20.568	−312.238	0.91575	0.65863	0.001551	1.906	
s-r-q2-Cu(O12)	20.823	−312.290	0.91383	0.66718	0.001726	1.903	
r-q2-Cu(O12,O14)	21.234	−323.949	0.93993	0.60938	0.002043	2.143	1.956
r-q1-Cu(O12,O14)	21.577	−323.552	0.94069	0.61724	0.002637	2.167	1.957
d-w-v1-Cu(O19)	21.841	−313.823	0.91484	0.53885	0.000455	1.960	
s-w-f2-Cu(O12)	22.788	−312.261	0.90776	0.65286	0.000542	1.897	
r-q2-Cu(O8,O14)	23.842	−321.141	0.93716	0.60171	0.000663	2.171	1.949
r-q1-Cu(O8,O14)	24.729	−320.755	0.92884	0.57198	0.001635	2.119	1.951
s-w-Cu(O10,O19)	24.768	−310.281	0.88523	0.44781	0.000858	1.985	1.953
d-r-q2-Cu(O8)	24.806	−304.488	0.91525	0.59630	0.003204	1.906	
d-r-v1-Cu(O19)	24.898	−309.648	0.91404	0.53762	0.000452	1.964	
s-w-u-Cu(O8,O19)	28.485	−309.040	0.90694	0.28448	0.000397	2.165	2.002
d-r-q2-Cu(O12)	32.340	−296.984	0.92286	0.42172	0.000140	2.020	
s-w-u-Cu(O8,O19)-ξ	33.596	−296.589	0.89822	0.28475	−0.001278	2.185	1.984
s-r-Cu(O8,O19)	34.297	−298.509	0.89925	0.24325	0.000942	2.205	2.003
d-w-f1-a-Cu(O12)	34.831	−299.319	0.92554	0.43711	0.000065	1.023	
d-r-q2-Cu(O10)	35.569	−293.724	0.92657	0.73153	−0.002228	1.941	
d-r-f-1-a-Cu-O12	35.812	−297.308	0.92512	0.43984	0.000095	2.020	
d-r-q2-u-Cu(O12)	38.606	−293.949	0.94030	0.73558	0.000047	1.972	
s-r-q2-Cu(O8)	41.662	−291.451	0.92161	0.39759	0.000662	2.026	
d-w-v1-Cu(O10)	42.585	−291.566	0.94780	0.61575	−0.000231	2.004	
d-r-v1-Cu(O10)	43.000	−291.546	0.92649	0.74900	−0.000059	1.979	

Table 1 (continued)

Complex	Relative energy (kcal mol^{-1})	Molecule-ion interaction energy (kcal mol^{-1})	Charge on Cu in the complex		Cu atomic spin density (Mulliken)	Cu···O distance [a] (Å)	
			Natural	Mulliken		first O	second O
s-r-q1-Cu(O10)	43.587	−289.219	0.94074	0.72511	0.000972	1.999	
s-w-q1-Cu(O10)	46.935	−283.320	0.94557	0.44417	−0.001597	2.025	

[a] When the Cu ion is bonded to two O atoms, the first column reports the distance from the O atom mentioned first in the complex name, and the second column reports the distance from the other O atom.

[b, c,d, e,f,g,h, i] The Cu ion is also bonded to the C23═C24 double bond: [b] Cu···C23 is 2.075 and Cu···C24 is 2.271; [c] Cu···C23 is 2.076 and Cu···C24 is 2.278; [d] Cu···C23 is 2.075 and Cu···C24 is 2.272; [e] Cu···C23 is 2.865 and Cu···C24 is 2.071; [f] Cu···C23 is 2.070 and Cu···C24 is 2.275; [g] Cu···C23 is 2.107 and Cu···C24 is 2.261; [h] Cu···C23 is 2.101 and Cu···C24 is 2.269; [i] Cu···C23 is 2.101 and Cu···C24 is 2.262

appears in the complex, because there is nothing that can be matched to it among the stable conformers of isolated HPJ-A. On the other hand, the energy contribution of this IHB is not high: from comparison with analogous ACPLs where it is present [37], it is not expected to exceed 2.5 kcal mol^{-1}, which is not significantly influential compared to the MIIE values. An evaluation of a deformation-energy contribution as the difference between the closest stable conformer of isolated HPJ-A without the H20···O8 second IHB and the geometry that HPJ-A has in the complex, frozen to prevent changes, would be unrealistic because the H20···O8 second IHB appears to have stabilizing effects in the complex and destabilizing effects in isolated HPJ-A, and because IHB effects go beyond the conceptual domain of "deformation energy".

Both ΔE and MIIE values (Table 1) indicate that Cu^{2+} prefers to bind simultaneously to O19 and C23=C24, or to O19 and either O8 or O10, or only to C23=C24. This highlights an important role of the C23=C24 π bond in complex stabilization. A further preference for the O atoms in the region closer to COR (Cu^{2+} binding to O8 and O19 rather than to O10 and O19) may be due to the proximity to the C7=O14 π bond and the sp^2 character of O14. These features may also account for the fact that complexes in which Cu^{2+} binds to O14 are the only comparatively stable ones among those in which it binds to only one O atom.

The complex stability appears to be related also to the relative stabilities of the conformers of isolated HPJ-A and ACPLs in general [17]. Most low energy complexes are complexes of d-type conformers, with Cu^{2+} binding to its preferential sites, followed by complexes of s-w conformers. For instance, the stability of complexes in which Cu^{2+} binds only to O14 decreases along the conformer series d-r-q2, s-w-q1, d-w-f1, s-w-f2, s-r-q2, d-r-f1, s-r-q1. Second O8···O19 or O10···O19 IHBs have a stabilizing role in the complex, unless their breaking enables Cu^{2+} to bind to O8 and O9 or O10 and O19 simultaneously.

Complexes of HPJ-A high-energy conformers without the first IHB have rather good (but not the best) MIIE, but poor relative stability (high ΔE), consistent with the patterns of isolated HPJ-A and ACPLs in general. The Cu distance with O8 or O12 remains >2 Å, i.e., it is considerably longer than when Cu^{2+} binds to O19 and O8 or O10.

The possibility of O19−H20···π interaction (whose presence is identified by the symbol ξ in the complex names [63]) does not appear to favor complex stability, likely because the position of the C23=C24 π bond is not geometrically favorable, or because the interaction is less strong than with phenol OH, as considered in [63].

The natural charge of Cu in the complexes is reduced to +0.88 in the seven more stable complexes, and to the +0.83−0.96 range overall. The charge reduction appears to be related more to the binding site/s than to the MIIE. The lowest charge values pertain to complexes in which Cu binds to the C23=C24 π bond. The values are higher for complexes in which HPJ-A does not have the first IHB, despite their good MIIE.

The spin density on Cu becomes zero in the complexes, i.e., the spin density is located only on the HPJ-A moiety. The Cu electron configuration becomes d^{10}, confirming that

Table 2 Molecule ion interaction energy (MIIE, kcal mol^{-1}) corrected for ZPE, for representative complexes of hyperjovinol A with a Cu^{2+} ion. DFT/B3LYP results in vacuo with the 6-31+G (d,p) basis set for the C, O and H atoms and the LANL2DZ pseudopotential for Cu^{2+}, at 298.15 K and 1 atm

Complex	MIIE	Complex	MIIE	Complex	MIIE
d-w-v1-Cu(O19,pi)	−333.742	d-r-q2-Cu(O14)	−315.244	s-w-q1-Cu(O12)	−312.338
d-w-f1-Cu(O8,O19)	−333.330	s-w-q1-Cu(pi)	−315.302	w-q1-Cu(O12,O14)	−324.772
d-w-f2-Cu(O19,pi)	−331.769	d-w-f1-a-Cu(pi)	−318.312	s-r-q2-Cu(O14)	−313.937
d-r-v1-Cu(O19pi)	−330.056	s-w-q1-Cu(O14)	−314.736	s-r-q1-Cu(O14)	−312.879
d-r-f1-Cu(O8,O19)	−327.742	d-w-Cu(O10,O19)	−318.916	d-r-f1-a-Cu(O14)	−313.252
d-r-f1-Cu(O8O19)-ξ	−323.444	d-r-q2-Cu(O14)-b	−312.311	s-r-q1-Cu(O12)	−312.429
d-r-q2-Cu(pi)	−316.804	d-w-f1-a-Cu(O14)	−316.419	r-q2-Cu(O8,O14)	−320.994

Cu^{2+} is reduced to Cu^{+}. All these observations indicate an electron transfer from HPJ-A to the Cu ion. HPJ-A becomes a radical cation. The HOMO is singly occupied. The spin density is distributed mostly in the region/s away from the Cu binding site/s (Fig. 4) and completely away from the binding site when Cu binds to C23=C24.

The natural charge on the H atoms pertaining to the OH groups (H15, H16, H17 and H20), already≈0.5 in isolated HPJ-A, increases in the complex, mostly by 0.01–0.02 for H15, 0.01–0.03 for H16, 0.01–0.05 for H17 and 0.01–0.06 for H20. This can be viewed as part of the spreading through the HPJ-A moiety of the positive charge that it subtracts from the Cu ion. The natural charge on the O atoms becomes less negative (by 0.02–0.06/O14, 0.03–0.16/O8, 0.02–0.05/O10, 0.02–0.17/O12, 0.00–0.05/O19) when the Cu ion is not bonded to them and more negative (by 0.17–0.19/O14, 0.08–0.17/O8, 0.11–0.18/O10, 0.09–0.18/O12, 0.00–0.14/O19) when Cu is bonded to the given O.

The effects of complexation on the parameters of the ligand's IHBs depend on the site to which the Cu ion binds. When it binds to the C23=C24 double bond or to O10, both the first and the second IHB are significantly shortened. When Cu binds to O14, the first IHB length increases significantly. When Cu binds simultaneously to O8 and O19 or to O10 and O19, the first IHB length decreases if it engages H15 and increases if it engages H17. (The first IHB length is taken as H15···O14 or H17···O14 when there is no proton transfer in the complex, as H15···O8 or H17···O12 when there is a proton transfer).

Comparison of the results from calculations utilizing the LANL2DZ pseudopotential for the Cu^{2+} ion and from calculations utilizing B3LYP/6–31+G(d,p) for all the atoms show that trend-identifications from the latter are reliable. The complex relative stabilities sequence does not show significant differences; the only reversal cases concern high energy conformers ($\Delta E>16$ kcal mol^{-1}), and the difference between the ΔE whose positions are reversed is <0.67 kcal mol^{-1}. The ΔE gap between complexes is somewhat less in the LANL2DZ results, making ΔE values slightly smaller: by ≤0.55 for the complexes with $\Delta E<10.3$, by 1.1–1.9 for the others, and by 2.4–2.9 only for high energy complexes (($\Delta E>35$). The MIIE values are overestimated by calculations utilizing the 6–31+G(d,p) basis for all the atoms; however, the difference with the LANL2DZ results is fairly constant: 17.4–17.9 for the complexes with $\Delta E<10.3$, 15.2–16.8 for the others. The natural charges on Cu do not differ significantly; in most cases, the LANL2DZ results are 0.003–0.010 greater; they are slightly smaller (by 0.0004−0.0007) when Cu binds to both O19 and C23=C24. Mulliken charges on Cu differ more significantly, and are smaller in the LANL2DZ results, by 0.1–0.3 for the six lower energy complexes, and by 0.01–0.3 for the other complexes. For complexes in which Cu binds only to C23=C24, the LANL2DZ Mulliken charge is 0.03–0.10 greater. The absolute value of the Mulliken spin density on Cu is mostly 20–70 % smaller in the LANL2DZ results (although the values are close to 0 in both cases). The distance of Cu from the O atom/s to which it binds is 0.026–0.038 longer in the LANL2DZ results, which may be in line with the known tendency of pure DFT to give shorter distances for non-covalent interactions. The estimation of the IHB lengths is nearly always shorter in the LANL2DZ results, by 0.002–0.013 Å.

MIIE values corrected for ZPE (Table 2) do not differ substantially from those not including the correction (Table 1). The largest difference (1.922 kcal mol^{-1}) pertains to d-w-v1-Cu(O19,pi), followed by 1.60 for d-r-v1-Cu(O19pi) and 1.38 for d-w-f2-Cu(O19,pi). All the other differences are <1 kcal mol^{-1} and decrease to <0.5 kcal mol^{-1} (sometimes close to 0) for higher energy complexes.

Results for the complexes of the hyperjovinol A molecule in solution

Calculations in solution were performed for a representative selection of complexes: those with $\Delta E \leq 18$ kcal mol^{-1} and some complexes in which HPJ-A does not have the first IHB, to verify whether their ΔE changes significantly in water solution, as noted for ACPLs [17]. Table 3 reports data for most of the complexes calculated in solution: the ΔE values, the relative total free energy (ΔG), the charge on Cu ((both from natural population analysis and Mulliken), the Mulliken spin density on Cu, the free energy change of the solution process (ΔG_{solv}) and its electrostatic component (G_{el}). In the PCM method, ΔG_{solv} comprises an electrostatic component (G_{el}) and a non-electrostatic one; the latter includes the work required to build the cavity in the solvent to "host" the solute molecule.

PCM results are informative for aspects like the complex relative stabilities, the HPJ-A ability to reduce Cu^{2+} (through the charge and spin density on Cu), or the preference for one or another binding site (through complex ΔE), while they are less informative for MIIE.

The charge on Cu in a given complex is slightly greater in a solvent than in vacuo, but always remains below +1, indicating that the HPJ-A ability to reduce Cu^{2+} to Cu^{+} is maintained in all the solvents considered.

The complex relative stabilities show significant changes in the preferences for binding to the C23=C24 π bond, for O14 and for simultaneous binding to O10 and O19. The preference for simultaneous binding to O19 and C23=C24 increases in solution up to the point that d-w-f2-Cu(O19,pi) has considerably better ΔE than d-w-f1-Cu(O8,O19) in all the solvents, and d-r-v1-Cu(O19,pi) has considerably better ΔE in the non-protic solvents. Complexes where Cu^{2+} binds only to C23=C24 have considerably better ΔE in solution than those in which it binds to O14. The preference for O14

Table 3 Relevant quantities for representative complexes of hyperjovinol A with a Cu^{2+} cation in solution: complex relative energy (ΔE, kcal mol^{-1}), complex relative total free energy (ΔG, kcal mol^{-1}), charge on the Cu atom from natural population analysis (a.u.), Cu atom spin density (Mulliken), free energy of solution (ΔG_{solv}, kcal mol^{-1}) and its electrostatic component (ΔG_{el}, kcal mol^{-1}). PCM DFT/B3LYP results with the 6-31+G(d,p) basis set for the C, O and H atoms and the LANL2DZ pseudopotential for Cu. The solvents are denoted by chlrf (chloroform), actn (acetonitrile) and aq (water)

Complex	Solvent	ΔE	ΔG	Cu charge (natural)	Cu spin density	ΔG_{solv}	ΔG_{el}
d-w-v1-Cu(O19,pi)	chlrf	0.000	0.000	0.89521	−0.00004	−93.78	−98.61
	actn	0.000	0.000	0.90222	0.00014	−110.24	−122.88
	aq	0.349	0.392	0.91315	0.00012	−137.34	−146.12
d-w-f1-Cu(O8,O19)	chlrf	3.114	2.756	0.89552	0.02923	−92.49	−96.96
	actn	3.280	3.065	0.90627	0.03769	−108.63	−121.06
	aq	2.170	1.977	0.92690	0.05488	−137.22	−145.77
d-w-f2-Cu-(O19,pi)	chlrf	1.902	1.773	0.89183	0.00004	−93.87	−98.58
	actn	1.460	1.424	0.89892	0.00003	−110.67	−123.28
	aq	0.000	0.000	0.90845	0.00003	−139.60	−148.33
d-r-v1-Cu(O19,pi)	chlrf	2.538	2.629	0.89554	0.00025	−94.04	−98.96
	actn	2.512	2.578	0.90234	0.00018	−110.54	−123.25
	aq	3.118	3.214	0.91312	0.00017	−137.41	−146.24
d-r-f1-Cu(O8,O19)	chlrf	6.920	6.691	0.89811	0.02747	−109.76	−97.91
	actn	6.796	6.696	0.90878	0.03603	−93.30	−122.30
	aq	5.320	5.233	0.93029	0.05447	−138.72	−147.37
d-r-f1-Cu(O8,O19)-ξ	chlrf	9.853	9.967	0.91770	0.04445	−94.15	−99.10
	actn	8.691	8.830	0.92901	0.05247	−111.74	−124.52
	aq	7.011	7.269	0.93758	0.05739	−140.80	−149.79
d-r-q2-Cu(pi)	chlrf	12.935	13.611	0.86114	0.00001	−92.21	−97.72
	actn	13.138	14.022	0.87246	0.00001	−108.25	−121.78
	aq	12.958	13.980	0.89056	0.00002	−135.79	−145.55
d-r-q2-Cu(O14)	chlrf	20.708	21.270	0.94878	0.00001	−86.61	−92.01
	actn	22.959	23.751	0.95248	0.00003	−100.59	−114.02
	aq	23.533	24.547	0.95817	0.00007	−127.29	−137.04
s-w-q1-Cu(pi)	chlrf	13.618	15.190	0.88260	0.00014	−93.20	−99.61
	actn	13.421	15.073	0.89119	0.00016	−109.78	−124.07
	aq	13.535	15.564	0.90733	0.00019	−136.79	−147.55
d-w-f1-a-Cu(pi)	chlrf	15.929	17.279	0.88009	0.00050	−91.55	−97.73
	actn	16.080	17.674	0.88858	0.00048	−107.61	−121.85
	aq	13.444	15.350	0.90578	0.00050	−137.43	−148.07
s-w-q1-Cu(O14)	chlrf	20.976	22.214	0.95035	0.00001	−87.20	−93.28
	actn	22.642	23.992	0.95425	0.00002	−101.88	−115.88
	aq	23.827	25.527	0.96145	0.00007	−127.84	−138.28
d-w-Cu(O10,O19)	chlrf	13.892	13.618	0.89009	0.00234	−96.47	−101.03
	actn	12.209	12.108	0.89329	0.00290	−114.43	−126.98
	aq	8.279	8.234	0.89371	0.00321	−145.81	−154.50
d-r-q2-Cu-O14-b	chlrf	22.262	23.518	0.94763	0.00000	−87.15	−93.24
	actn	24.333	25.725	0.95078	0.00001	−101.40	−115.43
	aq	24.145	25.969	0.95621	0.00003	−128.65	−139.21
d-w-f1-a-Cu(O14)	chlrf	23.002	23.896	0.94720	0.00001	−87.69	−93.41
	actn	24.372	25.550	0.95062	0.00001	−102.49	−116.31
	aq	22.290	23.766	0.95636	0.00003	−131.77	−141.98
s-w-q1-Cu(O12)	chlrf	22.171	23.905	0.93146	0.00286	−87.97	−94.54
	actn	23.505	25.439	0.93859	0.00417	−102.89	−117.47
	aq	24.305	26.662	0.94956	0.00686	−129.16	−140.26

Table 3 (continued)

Complex	Solvent	ΔE	ΔG	Cu charge (natural)	Cu spin density	ΔG_{solv}	ΔG_{el}
w-q1-Cu(O12,O14)	chlrf	21.652	23.123	0.94703	0.00215	−89.37	−95.67
	actn	22.679	24.342	0.94884	0.00216	−104.60	−118.91
	aq	20.905	23.028	0.95222	0.00116	−133.42	−144.27
r-q2-Cu(O12,O14)	chlrf	24.102	25.065	0.94653	0.00169	−89.95	−95.75
	actn	25.163	26.414	0.94790	0.00128	−105.05	−118.95
	aq	23.245	24.843	0.95190	0.00042	−134.12	−144.46
r-q1-Cu(O12,O14)	chlrf	24.029	25.574	0.94712	0.00248	−89.78	−96.16
	actn	24.794	26.511	0.94830	0.00207	−105.30	−119.66
	aq	22.857	25.011	0.95163	0.00089	−134.30	−145.19
r-q2-Cu(O8,O14)	chlrf	25.228	26.264	0.94670	0.00084	−91.36	−97.23
	actn	26.005	27.322	0.94939	0.00082	−106.76	−120.72
	aq	24.303	25.980	0.95279	0.00035	−135.60	−146.01

decreases sharply in solution (higher ΔE) and the decrease is greater as the solvent polarity increases. The preference for simultaneous binding to O10 and O19 increases in solution and the increase is greater as the solvent polarity increases. The relative free energies in solution confirm this trend. The trends are consistent with the preference for the situation in which more OHs are available to form solute-solvent H-bonds [17] (although PCM does not, so far, take into account solute-solvent interactions for specific sites, like solute-solvent H-bonds, the ΔE, ΔG and ΔG_{solv} values provide indications about the solutes for which such interactions are stronger).

The charges on the O atoms vary only slightly from one medium to another. Some trends may be identified, like the charge on O14 becoming slightly more negative with increase in solvent polarity, when Cu binds to C23=C24.

The evaluation of MIIE in solution from purely PCM results, using Eq. (1), does not lead to close-to-reality values, because it does not take into account the desolvation contribution, which is relevant for the ligand and much more so for the cation, whose solvent-accessible surface decreases by a considerable proportion in the complex. Taking into account desolvation effects is not easy. In principle, it would require the possibility of reference situations for E_{ligand} and E_{ion} in which only the parts of the ligand and ion surfaces that remain solvent-accessible in the complex are considered in contact with the solvent. Furthermore, desolvation effects are different for different complexes − depending on the different ways in which Cu approaches the ligand − and this decreases the viability of MIIE comparisons across different complexes in the same medium. Therefore, the MIIE values in solution calculated from Eq. (1) serve merely as indications that the ligand-ion interaction is still strong in solution, but do not provide accurate estimations of the actual interaction strength. As predictable, the MIIE values decrease sharply as the medium polarity increases. The difference between medium-absence and medium-presence is the sharpest, 122–129 kcal mol^{-1} between in vacuo and in chloroform. The further decrease from chloroform to acetonitrile solution is 25–28 and from acetonitrile to water 34–38 kcal mol^{-1}.

The dipole moment trends show two main patterns: an increase with medium polarity, more frequent for complexes in which Cu binds to C23=C24 and O19, to C23=C24 alone or to O10 and O19 simultaneously; and a decrease from vacuum to chloroform to acetonitrile, followed by an increase in water, more frequent for the other complexes. Comparison of PCM single-point results with two PCM full-reoptimization test-cases shows that, while trends' identification is similar in both options, the individual values of dipole moments may differ considerably.

The values of ΔG_{solv} show that the solvent effect is greater when Cu binds to C23=C24 and O19, to C23=C24 alone, to O8 and O19 or to O10 and O19 (92–96/chlrf, 108–112/actn, 136–146/aq) and lower when it binds to other sites (87–91/chlrf, 101–107/actn and 127–136/aq), likely because the former options leave more OH free for interaction with the solvent.

Results for the calculated auxiliary structures

Although the prime responsibles for the antioxidant activity of polyphenols are the phenol OHs, other structural features characterizing individual molecules may contribute significantly. An attempt to investigate the possible influence of each relevant structural feature of HPJ-A for its antioxidant ability was carried out through comparisons with a number of auxiliary structures, each of them enabling better focus on specific features.

The auxiliary structures utilized are shown in Fig. 5. Structures B, D, E, F, G, M and M1 are meant to check the influence of the characteristics of R′ and of the bulk of R. Structures B and D check the influence of the position of O19–H20 in R′: in B, O19–H20 is closer to the benzene ring (attached to C17)

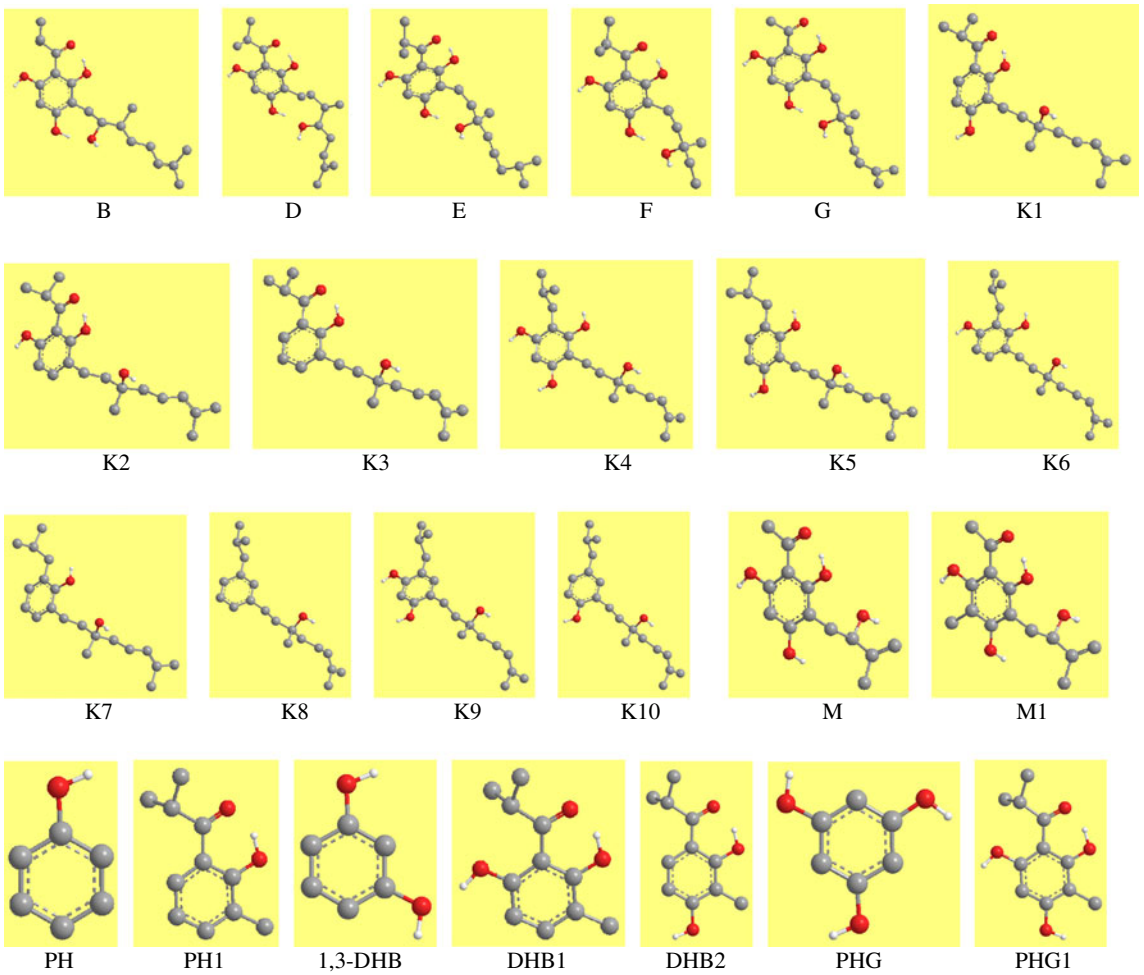

Fig. 5 The auxiliary structures utilized to investigate the influence of different structural features on the molecule's ability to bind and reduce the Cu^{2+} ion. The figure also shows the acronyms with which the structures are denoted on reporting results. The conformer shown for each structure is one of those utilized for complexes expected to have good molecule-ion interaction. All H atoms have been hidden except the phenol or alcohol ones. The skeletons correspond to full-optimization DFT/B3LYP/6–31+G(d,p) results in vacuo

and in D is further away (attached to C21) than in HPJ-A. Structure E checks the influence of the C23=C24 π bond at the end of R′, by removing it. F checks the influence of the length of R′, as it has a shorter R′, not including the double bond. G has a simpler R (CH_3, the simplest R≠H). In M, R′ is a prenyl chain, with O19–H20 attached to the first C of the double bond; it thus maintains the presence of both an OH and a π bond in R′, but with a different structural arrangement. M1 (included here because it had already been studied [37]) adds the presence of a methyl at C5.

Structures K1 to K10 check the effect of removing one or more of the phenol OHs, or also O14, while maintaining the same R′ as HPJ-A: removal of O12–H17 (K1), of O10–H16 (K2), of O12–H17 and O10–H16 (K3), of O14 (K4), of O14 and O12–H17 (K5), of O14 and O10–H16 (K6), of O14, O12–H17 and O10–H16 (K7), of O14, O8–H15, O12–H17 and O10–H16 (K8), of O14 and O8–H15 (K9) and of O14, O8–H15 and O12–H17 (K10).

A set of smaller structures is used to check the relevance of R′: the simplest hydroxybenzene (phenol, PH); 1,3-dihydroxybenzene (1,3-DHB); phloroglucinol (PHG, the parent compound of ACPLs); and corresponding structures with the same COR as HPJ-A and R′=methyl (PH1, DHB1, DHB2, and PHG1), where the methyl maintains the steric effects and conformational influences of the presence of R′≠H [17], but does not contain the additional OH and the π bond at the end of R′ which are likely involved in the antioxidant ability of HPJ-A.

Altogether, this selection enables a number of cross comparisons not only with HPJ-A, but also across pairs of auxiliary structures, to better elucidate possible roles of one or another feature. For the structures more closely related to HPJ-A (B, D, E, F, G), complexes with a Cu^{2+} ion corresponding to the best complexes of HPJ-A were calculated, both in vacuo and in solution: d-w-v1-Cu(O19,pi), d-w-Cu(O8,O19), d-r-Cu(O8,O19), d-r-q2-Cu(O14), d-w-Cu

Table 4 Comparison of the molecule-ion interaction energy for selected corresponding complexes of hyperjovinol A and of structures B, D, E, F and G. Results are from full optimization DFT/B3LYP calculations in vacuo, utilizing the 6–31+G(d,p) basis set for all the atoms. The nature of each structure is shown in Fig. 5

Complex	Molecule-ion interaction energy (kcal mol^{-1})					
	HPJ-A	B	D	E	F	G
d-w-v1-Cu(O19,pi)	−353.563	−357.575	−351.074	–[a]	–[a]	−350.957
d-w-Cu(O8,O19)	−350.107	−345.238	−347.837	−336.675	−335.995	−348.449
d-r-Cu(O8,O19)	−345.734	−338.875	−342.736	−331.480	−330.657	−342.635
d-r-q2-Cu(O14)	−331.316	−329.310	−325.222	−314.479	−312.968	−327.789
d-w-Cu(O10,O19)	−335.490	−331.351	−334.292	−326.089	−324.202	−328.297
s-w-q1-Cu(O14)	−330.665	−330.824	−323.960		−316.336	−327.612

[a] The d-w-v1-Cu(O19,pi) conformer is not possible for this structure because of the absence of the C=C double bond in R′

(O10,O19) and s-w-q1-Cu(O14). For structures K1 to K10, only a few representative complexes were calculated in vacuo, selecting those that enable comparisons with some complexes of HPJ-A or single out the influence of specific features. For the smaller structures, most or all the possible complexes were calculated (all the complexes of the lower energy conformers for PHG1). All the auxiliary structures were calculated with the 6–31+G(d,p) basis for all the atoms and, therefore, their results are compared with the results of HPJ-A from the same method.

The same atom-numbering (Fig. 1) is utilized for all the auxiliary structures, for discussing results. When some O atoms are not present in a given structure, the corresponding numbers are skipped, but the remaining atoms are still numbered as in Fig. 1, to facilitate comparisons across structures. Table 4 compares the MIIE for selected corresponding complexes of HPJ-A and of structures B, D, E, F and G. Table 5 shows the MIIE for the calculated complexes of the structures in which one or more OH of the phloroglucinol moiety, or O14, have been removed (structures K1 to K3). Table 6 reports the MIIE for the calculated complexes of the other structures utilized for additional comparisons (mostly, the smaller structures – PH, 1,3-DHB, PHG and the corresponding acylated structures).

For each complex-type, the complex of HPJ-A has better MIIE than the complexes of the other structures. The better MIIE than for B or D suggest that the position of O19H20 in R′ is optimal for HPJ-A. The fact that complexes where Cu binds to C23=C24 are best for HPJ-A, and the considerably better MIIE for the other complexes of HPJ-A than for those of E and F, suggest a significant role of the C2=C3 π bond. The MIIE of the complexes of E and F are close (somewhat better for E) and the charges on Cu are close, suggesting only minor influence by the length of R′ in the absence of the C=C π bond. The reduction of the charge of Cu is greater for the complexes of HPJ-A, with the only exception of few complexes of D. The Cu ion approaches the O atoms more closely in the complexes of HPJ-A than in those of the other structures, except for structure G, likely because of less steric hindrance by the smaller R. Comparison of M/M1 and B shows the importance of the distance of the π bond in R′ from the OH in R′, with the greater distance in B being more favorable. The complexes of G are those with closer

Table 5 Molecule ion interaction energy (MIIE, kcal mol^{-1}) for the calculated complexes of structures in which one or more OH of the phloroglucinol moiety, or O14, are removed. The structures are shown in Fig. 5

Complex[a]	MIIE	Complex	MIIE	Complex	MIIE
K1-d-w-Cu(O8,O19)	−347.119	K4-w-Cu(O8,O19)	−344.930	K6-Cu(pi)	−336.251
K1-d-w-Cu(O19,pi)	−345.310	K4-w-Cu(O10,O19)	−341.098	K7-Cu(O19,pi)	−348.780
K1-d-w-Cu(pi)	−329.664	K4-w-Cu(pi)	−340.690	K7-Cu(O8,O19)	−334.618
K2-d-Cu(O19,pi)	−351.539	K4-r-Cu(O8,O19)	−338.773	K8-Cu(O19,pi)	−335.945
K2-d-Cu(O8,O19)	−348.065	K5-w-Cu(O19,pi)	−356.772	K8-Cu(pi)	−318.980
K2-d-Cu(pi)	−335.235	K5-w-Cu(O10,O19)	−340.413	K9-w-Cu(O19,pi)	−357.566
K3-d-Cu(O8,O19)	−342.914	K5-w-Cu(pi)	−337.701	K9-w-Cu(pi)	−339.595
K3-d-w-Cu(O19,pi)	−342.841	K5-w-Cu(O8,O19)	−336.232	K9-w-Cu(O10,O19)	−337.980
K3-d-Cu(pi)	−327.597	K6-Cu(O19,pi)	−353.349	K10-w-Cu(O19,pi)	−350.306
K4-w-Cu(O19,pi)	−359.270	K6-Cu(O8,O19)	−340.067	K10-w-Cu(O10,O19)	−333.192

[a] For molecules with smaller number of O atoms, the number O14 is maintained for the sp^2 O of the acyl chain and the number O8 for the O of the OH in ortho to it and on the side of R′, to facilitate comparisons across structures

Table 6 Molecule ion interaction energy (MIIE, kcal mol^{-1}) for the calculated complexes of other structures utilized for additional comparisons. The structures are shown in Fig. 5

Complex[a]	MIIE	Complex	MIIE	Complex	MIIE
PH-Cu(O)	−238.192	DHB1-d-Cu(O14)	−293.594	PHG-b-Cu(O)	−258.804
PH1-Cu(O14)	−281.290	DHB1-d-Cu(O8)	−286.349	PHG-b-Cu(ar)[b]	−254.333
PH1-Cu(O8)	−275.764	DHB2-d-w-a-Cu(O14)	−285.838	M-d-w-Cu(O8,O19)	−320.162
1,3-DHB-b-Cu(O)	−254.260	DHB2-d-w-a-Cu(O8)	−279.293	M-d-r-Cu(O8,O19)	−314.567
1,3-DHB-a-Cu(O)	−252.887	PHG-a-Cu(O)	−258.220	B-Y3B5-Cu(O8,O19)	−322.099
1,3-DHB-b-Cu(ar)[b]	−248.880				

[a] For molecules with smaller number of O atoms, the number O14 is maintained for the sp^2 O of the acyl chain and the number O8 for the O of the OH in ortho to it and on the side of R′, to facilitate comparisons across structures

[b] In this case, the Cu^{2+} ion appears to interact preferably with the π system of the benzene ring. It binds to the C atom between the two OH

values to those of HPJ-A, suggesting that the influence by the nature and bulk of R is less important than the other factors.

Comparison of the PH/PH1, 1,3-DHB/DHB1, 1,3-DHB/DHB2 and PHG/PHG1 pairs (Table 6) highlights the role of the COR group. Its presence increases the MIIE for binding to a phenol O by 37 kcal mol^{-1} in the PH/PH1 pair, by 32 kcal mol^{-1} in the 1,3-DHB/DHB1 and 25 kcal mol^{-1} in the 1,3-DHB/DHB2 pairs, and by 15 kcal mol^{-1} for O8 and 31 kcal mol^{-1} for O10 in the PHG/PHG1 pair. Moreover, the sp^2 O of COR is an additional and more favorable binding site, yielding better MIIE and better Cu charge decrease than when Cu^{2+} binds to a phenol O. This suggests that ACPLs may be better candidates for antioxidant drugs than polyphenols without a COR group.

Steric hindrances may somewhat hinder a closer approach of Cu^{2+} to the O to which it binds. In PHG1, R′= methyl hinders the approach of Cu^{2+} to O10 in w conformers. The isopropyl in COR hinders the approach of Cu^{2+} to O12 in d-r conformers.

Comparison of the K-series structures (Table 5) points to some possible patterns, but deeper investigation (calculation of more complexes) would be needed to reach more conclusive inferences (it may be the object of a separate work). The effect of Cu binding to C23=C24 appears rather independent of the presence of the phenol OHs and O14: the MIIE for Cu(O19,pi) complexes is better in K4, K5 and K9 than in HPJ-A; the MIIE for Cu(pi) complexes is better in K4, K5, K6 and K9 than in HPJ-A. Conversely, Cu binding to at least one O of phenol OH is influenced by the presence of the other OH and O14: e.g., the MIIE for Cu(O8,O19,pi) complexes is better in HPJ-A than in any of the K structures.

Conclusions

The work modeled the antioxidant ability of HPJ-A through its ability to coordinate and reduce a Cu^{2+} ion. Although the work is not exhaustive in terms of possible complexes of HPJ-A with a Cu^{2+} ion, the number of calculated complexes, the fact that all possible complexes of the lower energy conformers of HPJ-A have been calculated, and the fact that the calculation of new complexes of higher energy conformers of HPJ-A regularly yields complexes with poorer ΔE and poorer MIIE, support the reliability of deriving inferences from the results obtained.

The model accounts for the HPJ-A antioxidant ability through the good MIIE and through the reduction of the Cu ion charge in the complexes. The preference of Cu^{2+} to bind to O19 and C23=C24, to C23=C24 alone, or simultaneously to O8 and O19 or to O10 and O19, suggests an important role of R′ for the antioxidant ability of HPJ-A. The results in solution, above all in non-polar or medium-polarity solvents, suggest that HPJ-A maintains its ability to reduce Cu^{2+} also when in a medium.

Comparison with the complexes of other structures selected to "isolate" the influence of one or another structural feature suggests that the HPJ-A molecule has a more convenient combination of structural features favoring antioxidant ability: the presence and position of the OH in R′; the presence and position of the π bond in R′; the nature of R; and the presence of the ACPL moiety. The synergic effects of such combination likely account for the good experimental antioxidant activity of HPJ-A.

The obtained results also suggest the opportunity of additional separate studies, like that of the keto-enol tautomerism between O14 and O8 or O12, or a comparison of the performance of B3LYP and BHLYP for these complexes. However, such studies would benefit from the inclusion of other ACPL molecules and, therefore, will be conducted at a later stage.

Acknowledgments The author expresses her gratitude to Prof. Maurizio Persico, of the Department of Chemistry and Industrial Chemistry of the University of Pisa (Italy), for his technical assistance, and to Dr. Caterina Ghio and Dr. Giuliano Alagona, of the Institute for Physico-Chemical Processes – Molecular Modelling Lab (Pisa), for fruitful interactions.

References

1. Athanasas K, Magiatis P, Fokialakis N, Skaltsounis AL, Pratsinis H, Kletsas D (2004) J Nat Prod 67:973–977
2. Singh IP, Bharate SB (2006) Nat Prod Rep 23:558–591
3. Peuchen S, Bolanos JP, Heales SJR, Almeida A, Duchen MR, Clark JB (1997) Prog Neurobiol 52:261–281
4. Facchinetti F, Dawson VL, Dawson TM (1998) Cell Mol Neurobiol 18:667–677
5. Alagona G, Ghio C (2009) Phys Chem Chem Phys 11:776–790
6. Chiodo SG, Leopoldini M, Russo N, Toscano M (2010) Phys Chem Chem Phys 12:7662–7670
7. Leopoldini M, Prieto Pitarch I, Russo N, Toscano M (2004) J Phys Chem A 108:92–96
8. Leopoldini M, Marino T, Russo N, Toscano M (2004) J Phys Chem A 108:4916–4922
9. Leopoldini M, Marino T, Russo N, Toscano M (2004) Theor Chem Acc 111:210–216
10. Leopoldini M, Russo N, Toscano M (2006) J Agric Food Chem 54:3078–3085
11. Leopoldini M, Russo N, Toscano M (2007) J Agric Food Chem 55:7944–7949
12. Leopoldini M, Russo N, Toscano M (2011) Food Chem 125:288–306
13. Leopoldini M, Chiodo SG, Russo N, Toscano M (2011) J Chem Theory Comput 7:4218–4233
14. Bentes ALA, Borges RS, Monteiro WR, Luiz G. M. de Macedo LGM, Alves CN (2011) Molecules 16: 1749–1760
15. Iuga C, Alvarez-Idaboy JR, Russo N (2012) J Org Chem 77:3868–3877
16. Verotta L (2003) Phytochem Rev 1:389–407
17. Kabanda MM., Mammino L (2012) Int J Quant Chem, doi:10.1002/qua.24012
18. Mammino L, Kabanda MM (2009) J Mol Struct (THEOCHEM) 901:210–219
19. Mammino L, Kabanda MM (2009) J Phys Chem A 113 (52):15064–15077
20. Alagona G, Ghio C (2009) J Phys Chem A 113:15206–15216
21. Bryantsev VS, Diallo MS, Goddard WA III (2009) J Phys Chem A 113:9559–9567
22. Bertrán J, Rodríguez-Santiago L, Sodupe M (1999) J Phys Chem B 103:2310–2317
23. Sabolović J, Tautermann CS, Loerting T, Liedl KR (2003) Inorg Chem 42(7):2268–2279
24. Hattori T, Toraishi T, Tsuneda T, Nagasaki S, Tanaka S (2005) J Phys Chem A 109:10403–10409
25. Georgieva I, Trendafilova N, Rodríguez-Santiago L, Sodupe M (2005) J Phys Chem A 109:5668–5676
26. Marino T, Toscano M, Russo N, Grand A (2006) J Phys Chem B 110:24666–24673
27. Rimola A, Rodríguez-Santiago L, Ugliengo P, Sodupe M (2007) J Phys Chem B 111:5740–5747
28. Lamsabhi AM, Alcamí M, Mó O, Yáñez M (2003) ChemPhysChem 4:1011–1016
29. Lamsabhi AM, Alcamí M, Mó O, Yáñez M, Tortajada J (2004) ChemPhysChem 5:1871–1878
30. Lamsabhi AM, Alcamí M, Mó O, Yáñez M, Tortajada J (2006) J Phys Chem A 110:1943–1950
31. Lamsabhi AM, Alcamí M, Mó O, Yáñez M, Tortajada J, Salpin JY (2007) ChemPhysChem 8:181–187
32. Noguera M, Bertrán J, Sodupe M (2008) J Phys Chem B 112:4817–4825
33. Rickard GA, Gomez-Balderas R, Brunelle P, Raffa DF, Arvi Rauk A (2005) J Phys Chem A 109:8361–8370
34. Becke AD (1992) J Chem Phys 96:9489
35. Becke AD (1993) J Chem Phys 98:5648–5652
36. Lee C, Yang W, Parr RG (1998) Phys Rev B 37:785–789
37. Mammino L, Kabanda MM (2012) Molec Simul doi:10.1080/08927022.2012.700483
38. Hay J, Wadt WR (1985) J Chem Phys 82(270):284–299
39. Siegbahn PEM (2003) Quarterly Rev Biophysics 36(1):91–145
40. Siegbahn PE (2006) J Biol Inorg Chem 11(6):695–701
41. Poater J, Solà M, Rimola A, Rodríguez-Santiago L, Sodupe M (2004) J Phys Chem A 108:6072–6078
42. Leopoldini M, Chiodo S, Russo N, Toscano M (2006) J Agric Food Chem 54:6343–6351
43. Belcastro M, Marino T, Russo N, Toscano M (2006) Theor Chem Acc 115:361–369
44. Reed AE, Weinhold F (1983) J Chem Phys 78(6):4066–4074
45. Reed AE, Weinhold F (1985) J Chem Phys 83(4):1736–1741
46. Reed AE, Weinstock RB, Weinhold F (1985) J Chem Phys 83 (2):735–747
47. Carpenter JE, Weinhold F (1988) J Molec Struct (Theochem) 169:41–62
48. Reed AE, Curtiss LA, Weinhold F (1988) Chem Rev 88(6):899–926
49. Hertwig RH, Koch W, Schroder D, Schwarz H, Hrusak J, Schwerdtfeger P (1996) J Phys Chem 100:12253–12260
50. Tomasi J, Persico M (1994) Chem Rev 94:2027–2094
51. Tomasi J, Mennucci B, Cammi R (2005) Chem Rev 105:2999–3093
52. Frisch MJ, Trucks GW, Schlegel HB, Scuseria GE, Robb MA, Cheeseman JR, Montgomery JA, Vreven T, Kudin KN, Burant JC, Millam JM, Iyengar SS, Tomasi J, Barone V, Mennucci B, Cossi M, Scalmani G, Rega N, Petersson GA, Nakatsuji H, Hada M, Ehara M, Toyota K, Fukuda R, Hasegawa J, Ishida M, Nakajima T, Honda Y, Kitao O, Nakai H, Klene M, Li X, Knox JE, Hratchian HP, Cross JB, Adamo C, Jaramillo J, Gomperts R, Stratmann RE, Yazyev O, Austin AJ, Cammi R, Pomelli C, Ochterski JW, Ayala PY, Morokuma K, Voth GA, Salvador P, Dannenberg JJ, Zakrzewski VG, Dapprich S, Daniels AD, Strain MC, Farkas O, Malick DK, Rabuck AD, Raghavachari K, Foresman JB, Ortiz JV, Cui Q, Baboul AG, Clifford S, Cioslowski J, Stefanov BB, Liu G, Liashenko A, Piskorz P, Komaromi I, Martin RL, Fox DJ, Keith T, Al-Laham MA, Peng CY, Nanayakkara A, Challacombe M, Gill PMW, Johnson B, Chen W, Wong MW, Gonzalez C, Pople JA (2003) GAUSSIAN 03, version D 01. Gaussian, Inc., Pittsburgh
53. Mennucci B, Tomasi J (1997) J Chem Phys 106:5151–5158
54. Mennucci B, Cancès E, Tomasi J (1997) J Phys Chem B 101:10506–10517
55. Cancès E, Mennucci B, Tomasi J (1997) J Chem Phys 107:3032–3041
56. Barone V, Cossi M, Tomasi J (1998) J Comput Chem 19:404–417
57. Siboulet B, Marsden CJ, Vitorge P (2006) Chem Phys 326:289–296
58. Bryantsev VS, Diallo MS, van Duin ACT, Goddard WA (2008) J Phys Chem A 112:9104–9112
59. Bryantsev VS, Diallo MS, Goddard WA (2008) J Phys Chem B 112:9709–9719
60. Spoliti M, Bencivenni L, Quirante JJ, Ramondo F (1997) J Mol Struct (THEOCHEM) 390:139–148
61. Gilli P, Bertolasi V, Ferretti V, Gilli G (1994) J Am Chem Soc 116:909–915
62. Sanz P, Mó O, Yañez M, Elguero J (2007) J Phys Chem A 111 (18):3585–3591
63. Mammino L, Kabanda MM (2012) Int J Quant Chem 112:2650–2658